J Exp Biol Advance Online Articles. First posted online on 29 May 2015 as doi:10.1242/jeb.118604
Access the most recent version at http://jeb.biologists.org/lookup/doi/10.1242/jeb.118604

Sensory processing within antenna enables rapid implementation of feedback control for high-speed running maneuvers

Jean-Michel Mongeau[1], Simon N. Sponberg[2,3], John P. Miller[4], Robert J. Full[2]

[1] *Biophysics Graduate Group, University of California – Berkeley, Berkeley, CA 94720-3220, USA*

[2] *Department of Integrative Biology, University of California – Berkeley, Berkeley, CA 94720-3140, USA*

[3] *Department of Biology, University of Washington, Seattle, WA 98195-1800, USA*

[4] *Center for Computational Biology, Montana State University, Bozeman, MT 59717-3148, USA*

Author for correspondence: J-M Mongeau, Howard Hughes Medical Institute, UCLA Department of Integrative Biology and Physiology, 2014 Terasaki Life Sciences Bldg, 610 Charles Young Dr. East, Los Angeles, CA 90095-7239 (email: jmmongeau@ucla.edu).

ABSTRACT

Animals are remarkably stable during high-speed maneuvers. As the speed of locomotion increases, neural bandwidth and processing delays can limit the ability to achieve and maintain stable control. Processing the information of sensory stimuli into a control signal within the sensor itself could enable rapid implementation of whole-body feedback control during high-speed locomotion. Here, we show that processing in antennal afferents is sufficient to act as control signal for a fast sensorimotor loop. American cockroaches *Periplaneta americana* use their antennae to mediate escape running by tracking vertical surfaces such as walls. A control theoretic model of wall following predicts that stable control is possible if the animal can compute wall position (P) and velocity, its derivative, (D). Previous whole-nerve recordings from the antenna during simulated turning experiments demonstrated a population response consistent with P and D encoding, and suggested that the response was synchronized with the timing of a turn executed while wall following. Here, we record extracellularly from individual mechanoreceptors distributed along the antenna and show that these receptors encode D and have distinct latencies and filtering properties. When summed, receptors transform the stimulus into a control signal that could control rapid steering maneuvers. The D encoding within the antenna in addition to the temporal filtering properties and P dependence of the population of afferents support a sensory encoding hypothesis from control theory. Our findings support the hypothesis that peripheral sensory processing can enable rapid implementation of whole-body feedback control during rapid running maneuvers.

INTRODUCTION

During high-speed running maneuvers, animals must rapidly integrate sensory information for whole-body stability. An outstanding challenge to reveal principles of sensorimotor control is to define how sensory information is processed to control body dynamics. Neural bandwidth limitations and delays can make stable, closed-loop control during high-speed running challenging because sensory information must be processed rapidly to direct whole-body dynamics (Cowan et al., 2006; Lee et al., 2008; Elzinga et al., 2012). Processing sensory stimuli at the earliest stage of sensorimotor integration could provide effective control if primary afferents transform stimuli into a control signal with little-to-no additional computation. The central nervous system of organisms, including invertebrates, can perform extensive processing of sensory stimuli (e.g. Borst and Theunissen 1999), but it requires time to do so. Less explored is the capability of primary afferents to not only encode, but also process sensory information to enable implementation of whole-body feedback control. By connecting sensing and body mechanics within a control theoretic framework, we can predict the type of processing needed to stabilize closed-loop behavior (Roth et al., 2014). Neuromechanical studies have revealed the importance of connecting sensory neural responses to the mechanical system they control (Chiel et al., 2009) as proposed in flying insects (Taylor and Krapp, 2007) and as demonstrated in chewing in sea slugs (Ye et al., 2006), swimming in lampreys (Ekeberg and Grillner, 1999), refuge tracking in electric fish (Cowan and Fortune, 2007) and flying in fruit flies (Dickson et al., 2006) and moths (Dyhr et al., 2013; Dickerson et al., 2014), but to our knowledge, no studies to date have linked sensory neural responses of primary afferents to the hypothesized requirements for whole-body control predicted by integrating the body within a control-theoretic framework. From the sensory encoding perspective, extraordinary efforts have described local, proprioceptive feedback circuits and afferent processing for controlling slow walking

behavior and posture (Duysens et al., 2000), such as in locusts (Matheson 1990; Kondoh et al., 1995; Holtje and Hustert, 2003; Zill and Jepson Innes, 1988), cockroaches (Ridgel et al., 2001; Spencer, 1974; Zill and Moran, 1981; Wong and Pearson,1976) and stick insects (Hess and Büschges 1997; Büschges and El Manira 1998; Zill et al., 2012; Zill et al., 2013), but it remains unclear to what extent afferent processing contribute to stabilize the whole-body during high-speed locomotion.

The American cockroach, *Periplaneta americana*, is an appropriate model system to study sensory processing as we have a well-developed understanding of its whole-body dynamics during rapid locomotion (Full and Tu, 1991; Holmes et al., 2006; Kubow and Full, 1999; Seipel et al., 2004). During tactilely-mediated rapid course control, termed "wall following", *P. americana* navigates using sensory feedback from the flagellum of its antenna to track surfaces at speeds up to 80 cm s^{-1} or 23 body lengths s^{-1} (Fig. 1A, C; Camhi and Johnson 1999). The antenna's flagellum has about 270,000 sensilla along its length that are sensitive to chemical and mechanical stimuli (Schafer and Sanchez 1973; Schaller 1978). The flagellum of *P. americana* has well-tuned mechanics for rapid course control. Reconfiguration of the flagellum mediated by chemo-mechanosensory hairs permits effective, rapid sensor orientation by passive mechanics (Mongeau et al., 2013). The flagellum's inelasticity keeps it in contact with objects after impact and thus isolates antennal bending events from inertial body motion, thereby increasing the reliability of tactile information (Mongeau et al., 2014). The flagellum's decreasing stiffness profile mechanically provides an effective look-ahead distance (Mongeau et al., 2014), a critical parameter to stabilize rapid running (Cowan et al., 2006). Finally, the flagellum's stiffness profile may simplify the transformation of flagellar bending to a single input, body-to-wall distance, by one-dimensional mapping (Mongeau et al., 2014). Wall projections, such as the animal encounters when going around a turn or negotiating a protrusion, bend the flagellum (Fig.

1C). As the flagellum bends, flagellar mechanoreceptors encode information allowing the cockroach to control its body angle to approach or move away from the surface (Camhi and Johnson 1999). *P. americana* can generate body rotations of up to 25 times per second and respond to impulse-like perturbations in as little as 30–40 ms (Camhi and Johnson 1999). These fast responses, combined with antennal conduction delays of 20 ms, as proposed by Camhi and Johnson (1999), suggest that neural delays impose severe constraints on control. In addition, at high-speeds the body of *P. americana* is inertial such that plant dynamics also impose important constraints on control (Holmes et al., 2006; Kubow and Full, 1999; Seipel et al., 2004). Thus, we hypothesize that cockroaches use sensory processing to implement feedback control during high-speed tactile navigation.

Whole-body dynamics have been integrated within a control model of cockroach high-speed wall following (Fig. 1A,B; Cowan et *al*., 2006; Lee et al., 2008). This model hypothesized that the cockroach controls its position *y* (sensed with antenna) by generating a control signal *u* proportional to turning torque in order to control its body (Fig. 1A,B). Incorporating a mechanical model with realistic running dynamics revealed that stable wall following with responses similar to natural behavior at different speeds requires a control signal that depends not only on the proportional (P) distance from the wall, but also wall velocity, the derivative (D) of position (Lee et al., 2008). In short, this control model predicts what sensory signal is required for stable running. In a prior study (Lee et al., 2008), it was hypothesized that at the level of mechanosensory afferents, processing of the antennal bending stimulus operates to match the information requirement for stable control of wall following.

As predicted from control theory, if mechanosensensory afferents are processing stimuli for enabling PD control, their responses would need to produce an output that has a similar time course to the control signal *u* or torque signal to control the body. Extracellular

tungsten recordings of the whole antenna nerve during a simulated turning experiment provided evidence of sensory processing at the level of primary afferents, both in terms of the time course of the neural response and the presence of PD-like encoding (Lee et al., 2008). Surprisingly, the response was sustained for ~300 ms after a brief 40 ms stimulus was concluded (Fig. 1D,E). Allowing for antennal conduction delays of approximately 20 ms, one would have expected the neural response to decay quickly following termination of the stimulus, declining within 60-80 ms. This persistence of the neural response does not match the time course of the stimulus. Instead, since the cockroach takes several strides (each ~70-100 ms) to complete a turn (Fig. 1C), we contend that this temporal filter in the antennal nerve transforms the sensory stimulus into a time course that matches the hypothesized control signal based on the animal's turn behavior. In addition to temporal filtering, the bulk population response was consistent with proportional (P) and derivative (D) control of wall position (Fig. 1D,E; Lee et al., 2008). Specifically, the root mean square (RMS) power of the neural response had directionally-dependent tonic and phasic components, respectively suggestive of P and D control. However, explicit encoding of velocity was not demonstrated and the question remains whether P and D signals are encoded at the level of individual receptors or the population.

Here, we took the next step to (1) determine if there are direct correlates of P and D signals in the primary afferents themselves that could implement the controller predicted by the control-theoretic model of wall following and (2) reveal how individual mechanosensors' responses sum to generate a processed population response. With respect to aim (1), we hypothesized that individual mechanoreceptive neurons *within* the antenna generate explicit P and D signals. Specifically, we predicted that spike rate would correlate with the position and velocity of an actuated wall segment used to simulate turning (Fig. 1F, H_{1b}). Alternatively, neural activity that directly correlates to P and D signals may be constructed downstream of

the antenna (Fig. 1F, H_{1a}). In this case, individual mechanoreceptors could encode features of wall movement from which P and D signals could be computed, but the signals would not be in a suitable representation for direct implementation of the controller. In this case, we would not predict an explicit correlation of P and D in the rate encoding of primary afferents and further processing in the brain would be required before the animal could implement a PD controller (Fig. 1F, H_{1a}).

With respect to our second aim (2), we hypothesized that each individual mechanoreceptive unit might have the same temporal filtering characteristics as the population response (Fig. 1F, H_{2a}). Alternatively, the population-level processing could arise from the combined action of multiple units each with its own unique delay and filtering property (Fig. 1F, H_{2b}). In this study, to test for evidence of processing in a hypothesized single-input-single-output behavior, we treat the components of the neuromechanical transform (e.g. the transform of individual mechanoreceptors) between the stimulus and neural response as an open-loop black box. We then link neural responses from individual primary afferents on the antenna flagellum to the hypothesized processing to stabilize a closed-loop, control theoretic model.

RESULTS

Derivative (D) encoding

To reveal the mechanism of sensory processing arising from individual primary afferents, we first examined P and D sensitivity and encoding in individual units (Fig. 1F, H_1). We bent the antenna with ethologically-relevant variable position and velocity steps, simulating a change in wall position, the putative signal that the animal is tracking during high-speed wall following ($r(t)$; Fig. 1A,B). We simultaneously recorded the activity of antennal receptors using an *en passant* suction electrode. From n = 46 identified units (19 recordings; N = 13 animals) for variable-velocity wall presentations, the majority of neuronal units (65%, 30/46) changed their firing rates in response to changing wall velocity, indicating D sensitivity (Kruskal-Wallis test, $\alpha<0.001$; Fig. 2A). The median number of detected units per recording for D-sensitive units was 2 (MIN = 1, MAX = 4). In 16/19 (84%) of preparations, at least one unit from the total identified units per recording was D sensitive. Our results show that the grand mean spike rate increased from 0 to ~60 spikes s^{-1} with a linear region from 0 to 60 mm s^{-1} (linear regression; t test for slope = 0, $p<0.001$) followed by a plateau (linear regression; t test for slope = 0, $p=0.252$) beyond a wall velocity of about 60 mm s^{-1}. The breakpoint near 60 mm s^{-1} was determined by searching for the point that minimizes the residual sum of squares using nonlinear regression for a two-line model (Jones and Molitoris, 1984). The broken-line or piecewise model was a marginally better fit than a single straight line (F test, DF=2, 6; p=0.05). When examining individual D-sensitive units, we identified 18 units with slopes significantly different from zero over the full range of velocities tested (linear regression t-test with $\alpha<0.001$), thus characterizing these units as D encoding and supporting hypothesis H_{1b} (Fig. 2B). For the average response of D-encoding

units, a piece-wise model was not a significantly better fit than a single line (*F* test, DF=2,6, p=0.13), suggesting that on average D-encoding units do not saturate at higher velocities.

From n = 54 identified units (N = 13 animals) for variable-position wall presentations, only two neurons from different animals (4%, 2/54) demonstrated position sensitivity where spike rate was different at any wall position (Kruskal-Wallis test, $\alpha<0.001$). However, we could not identify these units as P encoding because there was no significant correlation between wall position and spike rate (linear regression *t*-test with $\alpha<0.001$). Therefore, hypothesis H_{1b} is not supported for P.

Tuning of individual mechanoreceptors

To test the hypothesis that each individual neuron has the same temporal filtering property as the population response (Fig. 1F, H_{2a}), we characterized the properties of the neural response for each D-sensitive neural unit for the fastest wall velocity (trace of wall position and velocity shown Fig. 3Ai). When comparing across individual neural units, we determined variable unit responses to wall movements as evidenced by different delays to maximum firing rate, delays to first spike and decay rates (Fig. 3Aii, 3Bi), thus supporting hypothesis H_{2b}. Delay to maximum firing rate was highly variable (70 ± 21 ms; mean ± std unless otherwise specified) with a median of 77 ms (Fig. 3Bii). Similarly, we found a broad range of delays to first spike (range: 6.0 to 104 ms; 31 ± 25 ms) with a median of 23 ms (Fig. 3Biii). The median half-life from peak maximum rate for all neurons was 33 ms with some falling off very rapidly and others demonstrating sustained activity (range: 14 to 1160 ms; Fig. 3Ci–ii). In addition to the variable delays to maximum rate, delays to first spike and half-lives, we determined by visual inspection that one subset of neurons (approximately 11) exhibited large double peaks in their firing responses, corresponding to the periods of acceleration and deceleration of the wall (Fig. 5).

Temporal population processing from individual units

To reveal how individual units sum to generate the previously-observed processed population response reported in Lee et al. (2008), we first compared the normalized time course of each D-sensitive unit (Fig. 5) to the normalized population response (Fig. 1D). We found an average root mean square error (RMSE) of 0.25 and average R^2 of 0.24 between the normalized responses, indicating that individual units, on average, do not have the same response as the population response. To test if individual D-sensitive neural unit differences were sufficient to account for the population level processing, we summed the individual unit normalized responses and compared the summed time course to the normalized population response (Fig. 4). Summation of individual units (peak time = 100 ms; half-life = 150 ms; Fig. 3Aiii) approximated the temporal dynamics of the population response (peak time = 90 ms; half-life = 138 ms), with 87% of the variance (R^2) of the population response explained by the summation (RMSE = 0.09; Fig. 4), thus providing some assurance that our sampling distribution of units from multiple animals and recordings is adequate to approximate the total unit or true population response. To determine if the summed response was consistent with the presence of sustained, directionally-dependent tonic activity in the population, we compared the plateau regions of the response 1.0 to 1.5 s after stimulus onset (Fig. 4; plateau range not shown). The plateau region for the wall moving towards the animal was significantly more positive than the baseline firing rate (13% increase; paired *t*-test, $p<0.001$), suggesting sustained increases in firing rate well beyond the brief 70–80 ms stimulus. The plateau region of the spike rate for the wall moving away from the animal – following the wall moving towards the animal and holding for two seconds – was significantly more negative than the baseline spike rate (10% decrease; paired *t*-test, $p<0.001$). These shifts in plateau firing rates compared to baseline firing rates are consistent with position-dependent

tonic activity in the summed response of units, even though only a few units were explicitly position sensitive.

DISCUSSION

We discovered that individual mechanoreceptors along the antenna flagellum encode derivative (D) signals, sufficient for stable whole-body control at the first stage of sensory processing (Fig. 1F, H_{1b}). In addition, we revealed that both the position (P) dependence and the temporal filtering observed at the population level arises by these receptors having distinct latencies and filtering properties (Fig. 1F, H_{2b}). Together, these results provide evidence that sensory processing within the antenna itself can generate appropriate signal content and timing to enable effective implementation of feedback control for high-speed running.

Derivative (D) encoding

Our data support the hypothesis that individual mechanoreceptive neurons provide velocity encoding of a putative control signal generated from antennal bending, consistent with the D signal of the proposed PD controller of cockroach wall following (Fig. 1B). The identified D-sensitive neurons were sufficient to reconstruct the sensitivity to wall direction that was present in the whole-nerve population response (Fig. 4). We identified a small proportion of units with P sensitivity, but we could not statistically distinguish these as P-encoding. While it is possible that the few explicit P-sensitive units could be sufficient to yield the identified position dependence in the summed response, it is likely that smaller changes in tonic firing rate of D units that were not statistically distinguishable in isolation have aggregate effects when summed. In accord with this notion, we found that the summed

response of D-sensitive units was consistent with position-dependent tonic activity, based on shifts in plateau firing rate (Fig. 4). In summary, the identified population of receptive units on the antenna strongly supports the hypothesis that individual units encode D. While we found no evidence that individual units encode P, a P signal may be generated at the population level.

Here, we go beyond the first-level characterization of mechanoreceptors as phasic or phasic-tonic that can transduce kinematic variables such as position, velocity and/or acceleration of the stimulus. The control-theoretic framework allows us to test if the neural signals exiting the antenna enable implementation of whole-body feedback control for rapid turning. Based on previous characterizations of insect mechanoreceptors (Heinzel and Gewecke, 1979; Matheson 1990; Kondoh et al., 1995; Ridgel et al., 2001; Spencer, 1974; Zill and Moran 1981; Wong and Pearson, 1976; Hess and Büschges, 1997; Büschges and El Manira, 1998), it is expected that the receptors on the antenna would show phasic and phasic-tonic responses. However, what is surprising is that these mechanoreceptors can convey signals about a whole-body control variable at the level of primary afferents.

The neural responses of primary mechanoreceptive units in the flagellum are consistent with previous neurophysiological and morphological studies of mechanosensors in *P. americana*. For example, tactile hairs on the legs exhibit primarily phasic responses with rapid decay in firing rates in response to mechanical deflection (e.g. Spencer 1974). Direct stimulation of hair sensilla located on the trochanter (the leg segment between the coxa and femur) with varying-velocity ramp signals yields firing rates that scale linearly with velocity (Spencer 1974) then plateau, as we have observed on the antenna (Fig. 2B). It is known that there are a total of approximately 68,000 exteroceptive chemo/mechano-sensitive hair sensilla distributed along the flagellum of the cockroach *P. americana*, which represent about 25% of the total sensillum population (Schaller, 1978). Therefore, it is likely that the high

proportion of D-sensitive units with primarily *phasic* responses identified in this study are hair sensilla (Fig. 5). In contrast to exteroceptive sensors, sensors involved in proprioception, such as campaniform sensilla, have been shown to primarily exhibit phasic-tonic responses (Pringle 1938a; Pringle 1938b). On the antennal flagellum of *P. americana*, proprioceptive sensors are found in significantly smaller proportions compared to exteroceptive hair sensilla. According to a morphological study by Schafer and Sanchez (1973), there are fewer proprioceptive sensors than hair sensilla by about one order of magnitude, supporting the small number of phasic-tonic units identified in this study. Tibial campaniform sensilla in *P. americana* exhibit fast phasic responses with continued tonic activity (Zill and Moran, 1981) with the initial firing rate (phasic portion) dependent upon both the magnitude and direction of compressive forces. Just like phasic receptors, campaniform sensilla saturate beyond a range of velocities, as we have observed here (Ridgel et al., 2001). Finally, the identified phasic and phasic-tonic responses in our analysis are consistent with previous recordings of hair plate sensilla in *P. americana* located on the basal segment of the antennae (Okada and Toh, 2000; Okada and Toh 2001).

Tuning of individual mechanoreceptors by latency and temporal filtering

We discovered that mechanosensitive units along the antenna have distinct latencies and filtering properties to antennal bending. The majority of our measured latencies are within the expected range (0–50 ms) for action potentials traveling from mechanoreceptors distributed along the length of the flagellum (up to ~5 cm in length with a conduction velocity of 1–4 m s^{-1}; Pumphrey and Rawdon-Smith, 1937; Chapman and Pankhurst, 1967). Given that *P. americana* antennal axons have similar cross-sectional areas, without any known giant afferents (Baba and Comer 2008), the conduction velocities should be comparable, further supporting the argument that variable latencies arise at least, in part, from

the spatial distribution of sensors on the flagellum. However, some neurons' latencies (5 of 30) were longer than the 50 ms maximum expected simply due to conduction delays, indicating that sensilla location alone cannot account for the variation in unit latencies.

We determined a median latency-to-first-spike of 23 ms. Given that running cockroaches can respond to antennal touch within 30–40 ms during tactilely-mediated course control (Camhi and Johnson, 1999) suggests that neural delays from the antennal nerve impose severe constraints on control. Additional conduction delays between the antennal nerve and the thorax combined with muscle activation dynamic would appear to leave little time for processing. When these delays are combined with body dynamics, they could make it difficult to maintain stable control (Cowan et al., 2006; Lee et al., 2008; Elzinga et al., 2012). The 23 ms median latency we have measured is longer than the ~10 ms latency that has been measured by stimulating the antenna near its base and measuring activity in descending interneurons in cockroaches (Burdohan and Comer, 1990), stick insect (Ache and Durr, 2013) and crickets (Gebhardt and Honegger, 2001). We reason that this difference in latency is due to the location of stimulation as these studies deflected the basal segments of the antenna (scape and pedicel) while we displaced the antenna near its tip. Deflection near the tip maximally strains receptors at the tip due the antenna's exponentially decreasing stiffness profile (Mongeau et al., 2014).

Our results support the notion that antennal neurons have different filter functions between stimuli and responses (Fig. 1F, H_{2b}). The units with latencies above those expected due to conduction delays, along with the variable half-lives and the double maxima present in some neurons support this claim. These differences could arise neurally from encoding properties of different mechanoreceptors, or mechanically as a function of the local deformation at the sensors's location or material properties of each individual sensillum (Sane and McHenry 2009). Similar mechanisms have been proposed to explain phase shifts

between haltere mechanoreceptors in the crane fly (Fox et al., 2010). Further studies will need to address whether the variable-latency responses in *P. americana* antennae are due primarily to individual neurons' axonal conduction velocities, the spatial arrangement of mechanosensors, and/or individual mechanoreceptors' encoding properties. Revealing the biomechanical properties of the antenna can help to identify how mechanical filtering contributes to the overall processing at the level of afferents and control of wall following (Mongeau et al., 2013; Mongeau et al., 2014; Staudacher et al., 2005). While characterization of specific mechanoreceptor populations on the antenna could identify further spatial organization, isolation of these neurons *via* backfilling is currently limited because of the long diffusion distances required (Nishino et al., 2005). Therefore, to our knowledge, the latest techniques in retrograde filling are inadequate to sample a broad population of mechanoreceptors, as we have done here with extracellular recordings. To uncover the mechanism of population-level processing, a next step will be to determine the location and type of mechanoreceptors. However, knowing the location and type of receptors alone will be insufficient. It will also be necessary to reveal how mechanical forces are transmitted along the antenna, individual mechanoreceptors' transform, and axonal conduction velocities. One important avenue of future research will be to uncover the individual components of the neuromechanical transform, which we have treated as a black box for system analysis.

We identified some mechanosensitive units with encoding properties not predicted by the closed-loop PD control model of wall following (Fig. 1B). A significant proportion of the D-sensitive units (11/30) exhibited doubled peaks in firing rate corresponding to periods of wall acceleration and deceleration (or absolute value of acceleration). This indicates that for some units, acceleration signals may be provided at the level of afferents. While acceleration information is not necessary for a neural implementation of the control hypothesis from Lee et al. (2008), an acceleration signal could be implemented in a more elaborate controller for

wall following. The PD-control prediction from Cowan et al. (2006) cannot exclude the existence of a more complicated controller. Alternatively, acceleration may be irrelevant for wall following and may be used in other behaviors involving mechanosensation such as slower, active tactile exploration during object localization (Okada and Toh, 2000; Okada and Toh, 2001) or texture discrimination (Comer et al., 2003; Comer and Baba, 2014) and anemotaxis (Bell and Kramer 1979). Indeed, arthropod antennae are multifunctional sensory structures used in a variety of behaviors (Staudacher et al., 2005) where touch information can adjust the motor program in a context-dependent manner (e.g. Durr, 2001). Without the neuromechanical framework provided by a control theoretic hypothesis, it can be challenging to identify what information encoded by a sensor is relevant for a specific behavior.

Temporal population processing from individual neural units

We reject the hypothesis that mechanoreceptors are individually tuned to match the overall population response reported in Lee et al. (2008; Fig. 1F, H_{2a}). Instead, we discovered that the population-level processing of tactile information arises from the combined effect of many neurons with distinct latencies and filtering properties (Fig. 1F, H_{2b}; Fig. 3Bii, iii). The processed response from summed units starts with a rapid increase in firing rate, peaking near 100 ms, consistent with the timing of the onset of turning after the antenna starts to bend. This is followed by sustained tonic activity that extends well beyond the stimulus for about 300–500 ms, the approximate time it takes for the animal to complete a turn (Cowan et al., 2006; Lee et al., 2008).

Population-level processing from the summation of individually-tuned neurons is an established principle in system neuroscience whereby the coding properties of neurons are correlated to stimulus features, such as wind direction (Theunissen and Miller 1991), inertial forces (Fox et al., 2010) or visual motion direction (Maisak et al., 2013), and the individual

properties of neurons are compared across the sampled population to determine overall encoding. Here, we have extended the notion of population processing beyond the coding of the stimulus space; instead, we argue that primary afferent neurons may be tuned to transform the ethologically-relevant stimulus space into a processed control input to control the whole body with little-to-no further processing for effective sensorimotor integration. We contend that such transformation may be critical during rapid locomotion where incoming sensory signals must be rapidly combined with an ongoing motor program driving a dynamic body.

Revealing neural circuits involved in wall following and recording further downstream will provide insights into how this control signal is mapped onto existing motor patterns. For instance, recordings of units sensitive to antennal mechanical stimulation in the central complex (CC) of the cockroach *Blaberus discoidalis* suggest that some units downstream are velocity and acceleration sensitive (Ritzmann et al., 2008) and that CC activity is linked to locomotor changes, including turning behavior (Bender et al., 2010; Guo and Ritzmann 2013). However, it remains unclear whether these units' encoding properties are similar during dynamic tactile tasks such as high-speed tactile navigation, where both the body and the sensor are moving rapidly, or whether the neural circuit initiating rapid turning for wall following at all interfaces with the CC. The CC may serve as a motor planning region as suggested by Bender et al. (2010), executing the integration of controller signals into motor action. As downstream neural circuits are uncovered, an exciting avenue for future research will be to integrate the circuit-level description with control-theoretic models to better understand processing in neuromechanical systems.

MATERIALS AND METHODS

Animal preparation

We acquired adult male American cockroaches, *Periplaneta americana*, from a commercial vendor and housed them in plastic cages maintained at a temperature of 27 ºC. Cockroaches were exposed to a L:D cycle of 12h:12h and given fruits, dog chow and water *ad libitum*. We performed a total of 19 recordings (n = 13 animals, mass = 0.78 ± 0.13 g; right antenna length = 4.17 ± 0.38 cm; body length = 3.37 ± 0.16 cm; mean ± std unless otherwise specified) with some animals having two and at most three recordings at distinct locations. We sedated animals with intact antennae on ice for approximately 30 minutes. We restrained cockroaches dorsal side up on a Sylgard (Dow Corning Corporation) gel plate by placing insect pins in all six legs and one or two staple pins along the abdomen (Fig. 6). We placed an additional restraint pin between the pronotum and head such that the ventral side of the head was flush with the plate. We mechanically restrained the antenna of interest at an angle of 30° from the body midline. This is the angle that cockroaches typically maintain during wall following (Camhi and Johnson, 1999) and varies little (Mongeau et al., 2013). We fixed the region of the antenna covering the gel plate using epoxy glue that include the head-scape, scape-pedicel, and pedicel-flagellum joints. This preparation mechanically isolated the flagellum, which is necessary for turning during wall following (Camhi and Johnson, 1999), while preventing antennal and head movement.

To expose the base of the antennal nerve, we cut a small window through the cuticle on the dorsal side of the head. The auxiliary heart and antennal vessel were left intact thus preserving hemolymph exchange. Once the nerve was exposed, a petroleum-jelly well maintained a pool of cockroach saline around the nerve (Becht et al., 1960). After preparation, we mounted the animal at a distance of 2.5 cm from the body midline to the

actuated wall. The antenna was bent in an inverted J-shape characteristic of thigmotaxis in cockroaches (Camhi and Johnson, 1999; Cowan et al.,, 2006; Mongeau et al., 2013) and the distal-most segments were fixed to the wall with a small piece of wax to prevent the antenna from slipping laterally during our experiment.

Stimulus generation

To test our hypothesis about proportional (P) and derivative (D) encoding at the level of individual mechanoreceptors (Fig. 1F), we developed a system for precise position control, mimicking antennal displacements experienced during a turn while wall following (Cowan et al., 2006). Under natural processs, the antenna, in its backward-projecting configuration, experiences normal forces due to contact and little-to-no forces due to inertial body motion (Mongeau et al., 2014). Furthermore, the backward-projecting configuration the antenna can slide along the wall with little friction since the hairs are proximally-pointing and therefore in the direction opposite of motion. Therefore, the antenna's configuration reduces the probability of asperity-hair engagement to near zero (Mongeau et al., 2013). Consequently, axial and shear forces become very small. In contrast, normal contact forces dominate the antenna-wall interactions by causing the antenna to bend primarily in the lateral-medial plane. Therefore, to simulate the dominant region of the natural stimulus space, our stimulus was designed to bend the antenna in the lateral-medial plane. We attached an acrylic wall segment mounted to a plastic funnel that fit snugly around the cone of a larger speaker (Goldwood Sound, Inc., model GW-1248). We controlled wall position using the speaker's voice coil actuator driven by a current amplifier (LPAM-1, Quanser). To monitor the actual position output, a DC-DC Linear Variable Differential Transformer (LVDT; Trans-Tek Incorporated, model 0242-0000) was mounted parallel to the base of the wall. The current waveforms used to drive the speaker were generated using a custom Matlab script (Mathworks Inc.) and sent through a data acquisition board at 40,000 Hz.

Experimental protocol

We performed *en passant* extracellular suction recordings from the antennal nerve to sample from a broad population of mechanoreceptors and allow large mechanical deflections of the antennal nerve. Micropipettes (Sutter Instruments Co., model B150-86-10) were prepared using a custom recipe on a pipette puller (Sutter Instruments Co., model P-97) to form a short and gradual taper with diameter at the tip near 100 μm. Silver/Silver-chloride microelectrodes were mounted into the pipettes. The pulled pipettes had impedances less than 1 MΩ. A reference silver electrode was inserted in the saline pool, away from the recording site. Due to the anatomical orientation and size of antennal nerve (AN) 1, the main sensory nerve, our posterior approach allowed us to minimize interference from AN3-4 which innervate muscles at the base of the antenna (Baba and Comer, 2008). The distance between our recording electrode and sensory axonal units were probably on the order of micrometers while the distance between our recording electrode and the nearest efferent axons were on the order of ~100 μm. Given the approximate two-order of magnitude difference in distance between afferent and efferent axons, currents generated in AN3-4 by muscle activation would be on the order of 10^{-2} microvolts, thereby within the noise floor for spike detection. We were able to maintain stable recordings for about 3 hours with sufficient signal-to-noise to resolve individual units. Recordings were passed to a high input-impedance probe (Grass Instruments, HIZ probe) before filtering and amplification (Grass Instruments, P5 series AC pre-amplifier). Recordings were band-pass filtered from 100-10,000 Hz with a 60 Hz notch filter. Neurophysiological and LVDT position data were recorded simultaneously at a sampling rate of 40,000 Hz.

After we obtained a stable recording, we played variable position and velocity ramps through the actuated wall. In variable-position trials, position amplitudes ranged from 0.5-6 mm in steps of 0.5 mm, and the velocity was fixed at 1 mm s^{-1}. The variable-velocity ramps

ranged from 10 to 110 mm s^{-1} in steps of 10 mm s^{-1} and were fixed at a position of 10 mm. These ranges of positions and velocities are within the behaviorally-relevant range for wall following, as measured by Cowan et al., (2006) for a 30° turn while running at a rate of 7-17 strides s^{-1}. Each ramp was held at the desired position for a total of two seconds before returning to its neutral zero position for two seconds, thus corresponding to a sustained turning stimulus (Fig. 7). We randomized the presentation of variable position and velocity ramps. We collected a total of 10 trials per recording, which lasted for a total of about 1 hour. For the subsequent data analysis, the actual position outputs from the LVDT were used to analyze the neural response to position and velocity ramps. For each recording we performed a control experiment in which the antenna was not in contact with the wall while we played the ramp stimuli. This was to determine if chemo- or helio-sensitive receptors were activated during our experiments. We did not find effects of chemical or wind stimuli on our multi-unit recordings, likely because these axons are typically of much smaller diameter than mechanoreceptive units and were therefore in the noise floor of our recordings.

Data analysis

To identify and sort individual units from our extracellular recordings, we used supervised spike sorting based on wavelet decomposition and superparamagnetic clustering (SPC) algorithms developed by Quiroga et al. (2004; Fig. 8). Prior to processing, we digitally filtered the neural data with a 2^{nd} order Butterworth bandpass filter within a bandwidth of 3-20 kHz. To detect spikes we set a 1 ms absolute refractory period and used an amplitude threshold 5 times the estimated standard deviation of the background noise, as described by Quiroga et al., (2004). After detection, we stored a total of 3.2 ms of data for each spike. To cluster spikes, we used a total of 300 Monte Carlo iterations and set the minimum cluster size to 20 units. After a round of unsupervised clustering, we went through each individual trial to determine the quality of the clustering process by determining inter-trial repeatability and the

stability of the clusters over a range of clustering temperatures. We rejected individual trials within a recording session by determining the stability and reproducibility of clusters when compared to the average of trials within the same recording session. These outliers were detected infrequently (11/191 trials) and were most likely due to gradual loss in suction in the electrode during an individual recording.

To determine if individual units were responsive to the ramp stimuli, we computed a Gaussian-convolved firing rate from binary spikes using a Gaussian window with a standard deviation of 10 ms, thereby avoiding significant lags and maintaining an adequate temporal resolution (Fig. 8B,C). For variable-position ramp trials, we calculated the firing rate after the ramp reached its commanded position and was held; specifically, 0.5 s after and 0.5 s before it returned to its baseline position, for a total of 1.5 s. For variable-velocity ramp trials, we calculated the firing rate from the onset of the ramp to the point when it reached its final position. We computed the median firing rates during these intervals and subtracted these rates from the median baseline firing rate, which we computed over a 10 s interval after all ramp presentations for each recording.

To determine which units were responsive to our ramp stimuli, we used a non-parametric one-way analysis of variance test (Kruskal-Wallis) at a significance level of 0.001 between the Gaussian-convolved firing rates and the individual ramp positions and velocities. Only units responsive to variable-velocity ramps were used in the filtering and summation analysis. For these units, we measured the delays from the onset of a ramp presentation to the maximum spike rate and to the first spike. We measured the decay rates by computing the half-life from maximum Gaussian-convolved firing rates following the ramp presentation. Finally, we summed individual unit responses and compared the temporal characteristics of the summed response to the whole-nerve response reported in Lee et al. (2008). We summed the averages of each unit for multiple trials and report the grand mean. To determine if the

summed response was consistent with the presence of sustained tonic activity in some units, we compared the plateau regions of the response after stimulus onset. We defined the plateau region as 1.0 to 1.5 s after stimulus and the baseline as -0.5 to -0.1 s before stimulus.

AKNOWLEDGEMENTS

We thank Albert Kao for laboratory assistance as well as Jusuk Lee, Noah Cowan, Tom Daniel and Zane Aldworth for helpful discussions.

GRANTS

This research was funded by a National Science Foundation (NSF) Graduate Research Fellowship to J.-M.M., a NSF IGERT grant to PI R.J.F. and Fellowship to J.-M.M., a Fannie and John Hertz Foundation Fellowship to S.N.S., and a NSF FIBR grant to R.J.F. and J.P.M. (0425878).

REFERENCES

Ache, J.M., Durr, V. (2013). Encoding of near-range spatial information by descending interneurons in the stick insect antennal mechanosensory pathway. *J. Neurophysiol.* **110**: 2099–2112.

Baba Y., Comer C.M. (2008). Antennal motor system of the cockroach, *Periplaneta americana*. *Cell Tissue Res.* **331**: 751–762.

Becht G., Hoyle G., Usherwood P. (1960). Neuromuscular transmission in the coxal muscles of the cockroach. *J Insect Physiol.* **4**: 191–201,

Bell, W.J., Kramer, E. (1979). Search and anemotactic orientation of cockroaches. *J. Insect Physiol.* **25**: 631–640,

Bender J.A., Pollack A.J., Ritzmann R.E. (2010). Neural activity in the central complex of the insect brain is linked to locomotor changes. *Curr. Biol.* **20**: 921–926.

Borst A., Theunissen FE. (1999). Information theory and neural coding. *Nature Neurosci.* **2**: 947–957.

Burdohan, J.A., Comer, C.M. (1990). An antennal-derived mechanosensory pathway in the cockroach: descending interneurons as a substrate for evasive behavior. *Brain Res.* **10**: 347–352.

Büschges, A., El Manira, A. (1998). Sensory pathways and their modulation in the control of locomotion. *Curr. Opin. Neurobiol.* **8**: 733–739.

Camhi J.M., Johnson E.N. (1999). High-frequency steering maneuvers mediated by tactile cues: antennal wall-following in the cockroach. *J. Exp. Biol*. **202**: 631–643.

Chapman K., Pankhurst J. (1967). Conduction velocities and their temperature coefficients in sensory nerve fibres of cockroach legs. *J. Exp. Biol.* **46**: 63–84.

Chiel, H.J., Ting, L.H., Ekerberg, O., Hartmann, M.J.Z. (2009).The brain in its body: motor control and sensing in a biomechanical context. *J Neurosci.* **29**: 12807−12814.

Comer, C., Baba, Y. (2011). Active touch in orthopteroid insects: behaviors, multisensory substrates and evolution. *Phil. Trans. R. Soc. B.* **366,** 3006−3015.

Comer, C.M., Parks, L., Halvorsen, M.B., Breese-Terteling, A. (2003). The antennal system and cockroach evasive behavior. II. Stimulus identification and localization are separable antennal function. *J. Comp. Physiol. A* **189**: 97−103.

Cowan, N.J., Fortune, E..S. (2007). The critical role of locomotion mechanics in decoding sensory systems. *J. Neurosci.* **27**: 1123–1128.

Cowan N.J., Lee J., Full R.J. (2006). Task-level control of rapid wall following in the American cockroach. *J. Exp. Biol.* **209**: 1617–1629.

Cowan, N. J., Ankarali, M. M., Dyhr, J. P., Madhav, M. S., Roth, E., Sefati, S., Sponberg, S., Stamper, S.A., Fortune, E.S., Daniel, T. L. (2014). Feedback control as a framework for understanding tradeoffs in biology. *Integr. Comp. Biol*. **54**, 223–237.

Dickerson, B.H., Aldworth, Z.N., Daniel, T.L. (2014). Control of moth flight posture is mediated by wing mechanosensory feedback. *J. Exp. Biol.* **217**: 2301−2308.

Dickson, W.B., Straw, A.D., Poelma, C., Dickinson, M.H. (2006). An integrative model of insect flight control. *Proceedings of the Aerospace Sciences Meeting and Exhibit* 2006–2034.

Duysens, J., Clarac, F., Cruse, H. (2000). Load regulating mechanisms in gait and posture: comparative aspects. *Physiol. Rev.* **80**: 83–133.

Durr, V. (2001). Stereotypic leg searching-movements in the stick insect: Kinematic analysis, behavioural context and simulation. *J. Exp. Biol.* **204**: 1589-1604.

Dyhr, J.P., Morgansen, K.A., Daniel., T.L., Cowan, N.J. (2013). Flexible strategies for flight control: an active role for the abdomen. *J. Exp. Biol.* **216**: 1523-1536.

Ekeberg, O., Grillner, S. (1999). Simulations of neuromuscular control in lamprey swimming. *Philos. Trans. R. Soc. Lond. B Biol Sci* **354**: 895–902.

Elzinga M.J., Dickson W.B., Dickinson M.H. (2012). The influence of sensory delay on the yaw dynamics of a flapping insect. *J. R. Soc. Interface* **9**: 1685–1696.

Fox, J.L., Fairhall, A.L., Daniel T.L. (2010). Encoding properties of haltere neurons enable motion feature detection in a biological gyroscope. *PNAS* **107**: 3840–3845.

Full, R.J., Koditschek, D.E. (1999). Templates and anchors: neuromechanical hypotheses of legged locomotion on land. *J. Exp. Biol.* **202**: 3325–3332.

Full, R.J., Tu, M.S. (1991). Mechanics of rapid running insects: two-, four-, and six-legged locomotion. *J. Exp. Biol.* **156**: 215–231.

Gebhardt, M., Honegger, H.W. (2001). Physiological characterisation of antennal mechanosensory descending interneurons in an insect (*Gryllus bimaculatus, Gryllus campestris*) brain. *J. Exp. Biol.* **204**: 2265-2275.

Guo P., Ritzmann R.E. (2013). Neural activity in the central complex of the cockroach brain is linked to turning behaviors. *J. Exp. Biol.* **216**: 992–1002.

Heinzel, H.-G. and Gewecke, M. (1979) Directional sensitivity of antennal campaniform sensilla in locusts. *Naturwissenschaften* **66**:212–213.

Hess, D., Büschges, A. (1997). Sensorimotor pathways involved in interjoint reflex action of an insect leg. *J. Neurobio.* **33**: 891–913.

Holmes P., Full R.J., Koditschek D., Guckenheimer J. (2006). The dynamics of legged locomotion: models, analyses, and challenges. *SIAM Review* **48**: 207–304.

Hőltje, M. and Hustert., R. (2003) Rapid mechano-sensory pathways code leg impact and elicit very rapid reflexes in insects. *J. Exp. Biol.* **206**: 2715–2724.

Jones, R.H., Molitoris, B.A. (1984). A statistical method for determining the breakpoint of two lines. *Anal. Biochem.* **141**: 287–290.

Kondoh, Y., Okuma, J., Newland, P.L. (1995). Dynamics of neurons controlling movements of a locust hind leg: wiener kernel analysis of the responses of proprioceptive afferents. *J. Neurophys.* **73**: 1829–1842.

Kubow T. M. and R.J. Full, R.J. (1999). The role of the mechanical system in control: A hypothesis of self-stabilization in hexapedal runners. *Phil. Trans. Roy. Soc. London B.* **354**, 849-862.

Lee J., Sponberg S., Loh O.Y., Lamperski A.G., Full R.J., Cowan N.J. (2008). Templates and anchors for antenna-based wall following in cockroaches and robots. *IEEE Trans. Robot.* **24**: 130–143.

Maisak M.S., Haag J., Ammer G., Serbe E., Meier M., Leonhardt A., Schilling T., Bahl A., Rubin G.M., Nern A., Dickson B.J., Reiff D.F., Hopp E., Borst A. (2013). A directional tuning map of *Drosophila* elementary motion detectors. *Nature* **500**: 212–216.

Matheson, T. (1990). Responses and locations of neurones in the locust metathoracic femoral chordotonal organ. *J. Comp. Phys. A* **166**: 915–927**.**

Mongeau, J.-M., Demir, A., Lee, J., Cowan, N.J., Full, R.J. (2013). Locomotion- and mechanics-mediated tactile sensing: antenna reconfiguration simplifies control during high-speed navigation in cockroaches. *J. Exp. Biol.* **216**: 4530–4541.

Mongeau, J.-M., Demir, A., Dallmann, C.J., Jayaram, K., Cowan, N.J., Full, R.J. (2014). Mechanical processing *via* passive dynamic properties of the cockroach antenna can facilitate control during rapid running. *J. Exp. Biol.* **217**: 3333–3345.

Nishino H., Nishikawa M., Yokohari F., Mizunami M. (2005). Dual, multilayered somatosensory maps formed by antennal tactile and contact chemosensory afferents in an insect brain. *J. Comp. Neurol.* **493**: 291–308.

Okada J., Toh, Y. (2000). The role of antennal hair plates in object-guided tactile orientation in the cockroach *Periplaneta americana*. *J. Comp. Phys. A* **186**: 849–857.

Okada J., Toh Y. (2001). Peripheral representation of antennal orientation by the scapal hair plate of the cockroach *Periplaneta americana*. *J. Exp. Biol.* **204**: 4301–4309.

Pringle, J.W.S. (1938). Proprioception in insects. I. A new type of mechanical receptor from the palps of the cockroach. *J. Exp. Biol.* **15**: 101–113.

Pringle, J.W.S. (1938). Proprioception in insects. II. The action of the campaniform sensilla on the legs. *J. Exp. Biol.* **15**: 114–131.

Pumphrey R., Rawdon-Smith A. (1937). Synaptic transmission of nervous impulses through the last abdominal ganglion of the cockroach. *Proc. R. Soc. Lond. B. Biol. Sci*.**122**: 106–118.

Quiroga R.Q., Nadasdy Z., Ben-Shaul Y. (2004). Unsupervised spike detection and sorting with wavelets and superparamagnetic clustering. *Neural Comp.* **16**: 1661–1687.

Ridgel, A.L., Frazier, S.F., Zill, S.N. (2001). Dynamic response of tibial campaniform sensilla studied by substate displacement in freely moving cockroaches. *J. Comp. Phys. A* **187**: 405–420.

Ritzmann, R.E., Ridgel, A.L., Pollack, A.J. (2008). Multi-unit recording of antennal mechano-sensitive units in the central complex of the cockroach, *Blaberus discoidalis*. *J. Comp. Phys. A* **194**: 341–360.

Roth, E., Sponberg, S., Cowan, N.J. (2014). A comparative approach to closed-loop computation. *Curr. Opin. Neurobiol.* **25**: 54–62.

Sane, S.P., McHenry, M.J. (2009). The biomechanics of sensory organs. *Integr. Comp. Biol.* **49**: i8–i23.

Schafer R., Sanchez T.V. (1973). Antennal sensory system of the cockroach, *Periplaneta americana*: postembryonic development and morphology of the sense organs. *J. Comp. Neurol.* **149**: 335–354.

Schaller D. (1978). Antennal sensory system of *Periplaneta americana L*. *Cell Tissue Res* **191**: 121–139.

Seipel, J.E., Holmes, P.J., Full, R.J. (2004). Dynamics and stability of insect locomotion: a hexapedal model for horizontal plane motions. *Biol*. *Cyber*. **91**, 76-90.

Spencer, H.J. (1974). Analysis of the electrophysiological response of the trochanteral hair receptors of the cockroach. *J. Exp. Biol.* **60**: 223–240.

Staudacher E., Gebhardt, M., Durr V. (2005). Antennal movements and mechanoreception: neurobiology of active tactile sensors. *Adv*. *In Insect Phys.* **32**: 49–205.

Taylor, G.K., Krapp, H.G. (2007). Sensory systems and flight stability: what do insects measure and why? *Adv. In Insect Phys.* **34**: 231–316.

Theunissen, F.E., Miller, J.P. (1991). Representation of sensory information in the cricket cercal sensory system II. Information theoretic calculation of system accuracy and optimal tuning curve width of four primary interneurons. *J. Neurophys.* **66**: 1690–1703.

Ye, H., Morton, D.W., Chiel, **H.J**. (2006). Neuromechanics of multifunctionality during rejection in *Aplysia californica*. *J. Neurosci.* **26**: 10743–10755.

Wong, R.K., and Pearson, K.G. (1976). Properties of trochanteral hair plate and its function in control of walking in cockroach. *J. Exp. Biol.* **64**: 233–249.

Zill, S.N., Jepson Innes, K.A. (1988). Evolutionary adaptation of a reflex system: sensory hysteresis counters muscle 'catch' tension. *J. Comp. Physiol. A* **164**: 43–48

Zill, S.N., Moran, D.T. (1981). The exoskeleton and insect proprioception. I. Response of tibial campaniform sensilla to external and muscle-generated forces in the American cockroach, *Periplaneta americana*. *J. Exp. Biol.* **91**: 1–24.

Zill, S.N., Schmitz, J., Chaudhry, S., Buschges, A. (2012). Force encoding in stick insect legs delineates a reference frame for control. *J. Neurophys.* **108**: 1453-1472.

Zill, S.N., Chaudhry, S., Buschges, A., Schmitz, J. (2013). Directional specificity and encoding of muscle forces and loads by stick insect tibial campaniform sensilla, including receptors with round cuticular caps. *Arthropod Struct. Dev.* **42**: 455-467.

FIGURES

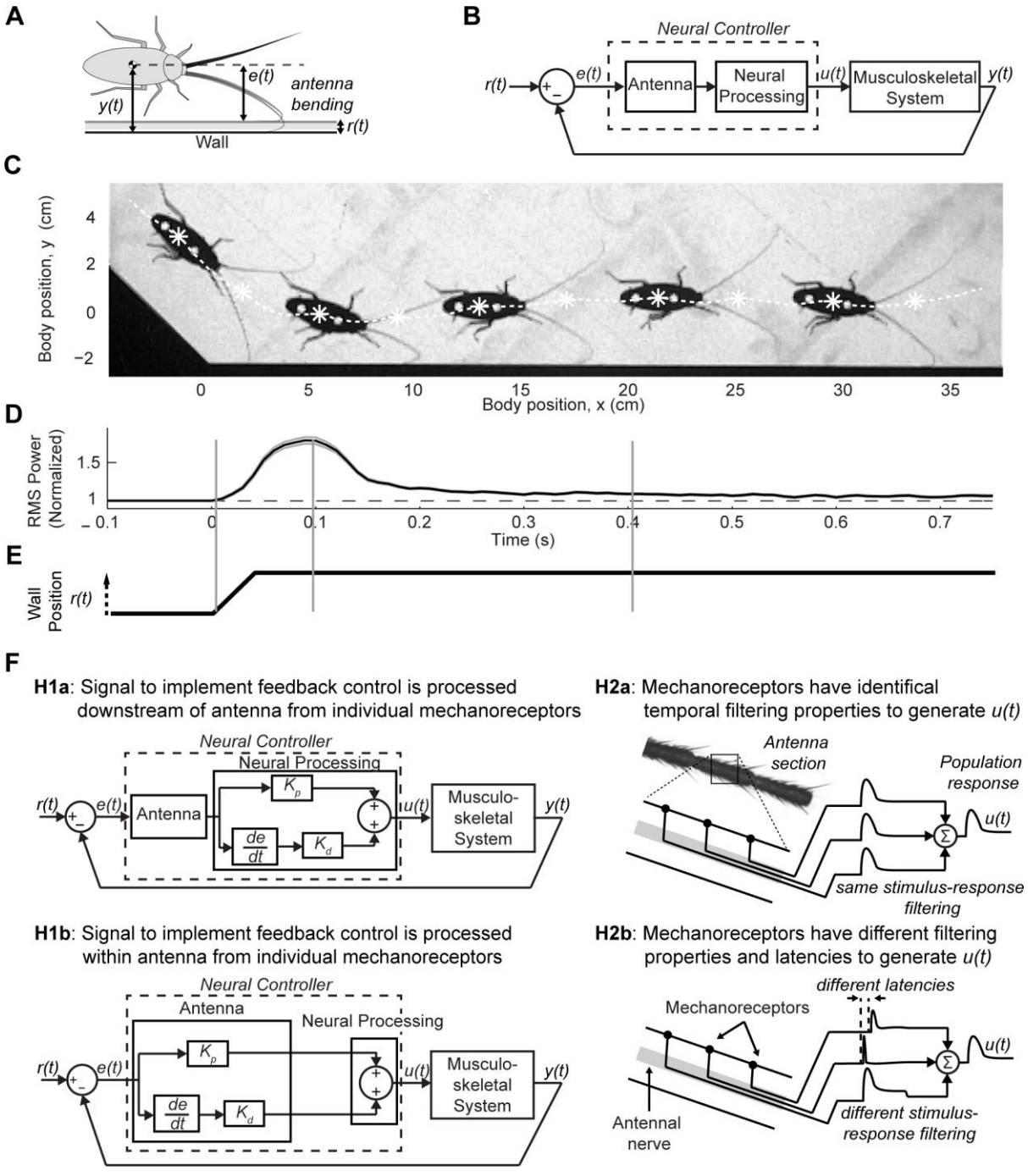

Figure 1. Biological control model and hypotheses. (A) Diagram of wall following cockroach. The cockroach controls its position *y(t)* relative to a global reference position of the wall *r(t)*. The error between these two signals is *e(t)*, an error signal generated by antennal

bending. (B) Control diagram of wall following where *u(t)* is the control input. This control model predicted that PD information provided by a neural controller is sufficient for stable wall following. P: Proportional. D: Derivative. (C) Sequence of turning as a blinded cockroach *P. americana* encounters a wall projection and responds to bending of the antenna. The dotted white line indicates the position of the point of rotation (POR) and asterisks indicate the initiation of a stride. (D) Bulk, population response from the antennal nerve. Despite a brief 40 ms ramp and hold wall stimulus (shown in E), activity was sustained for ~300 ms, matching the time course of the animal's turn behavior. Vertical lines indicate (from left to right) the onset of the wall movement, RMS peak time, and settling time. Adapted from Lee et al. (2008). (F) Neural control hypotheses. (Left column) We hypothesized that individual mechanoreceptors downstream (H1a; not tested here) or within the antenna (H1b) implement PD control by scaling the error signal *e(t)* proportional to a gain K_p and computing the derivative of *e(t)* with scaling by K_d. (Right column) We hypothesized that population-level processing arises from individual units having the same (H2a) or distinct (H2b) stimulus-response filtering to generate a population response *u(t)*.

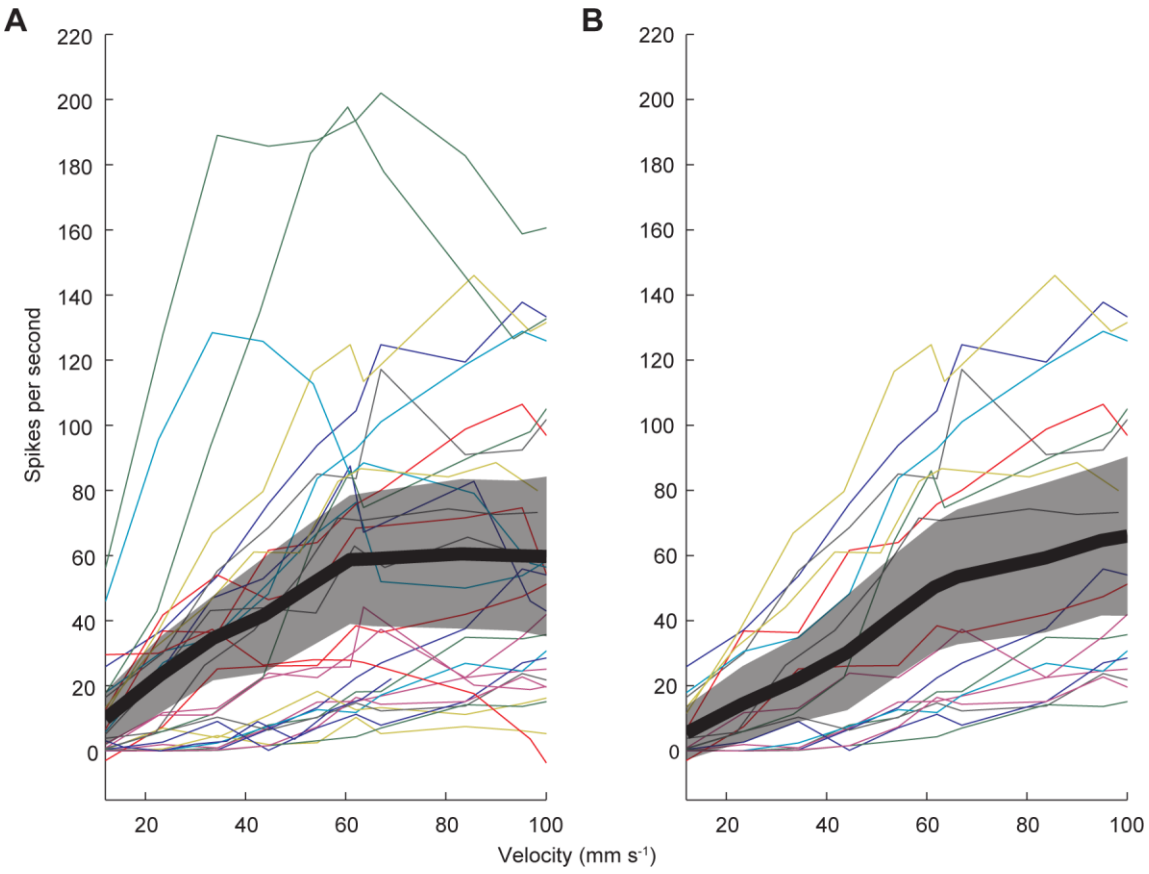

Figure 2. Derivative (D) encoding of individual neurons. (A) Neural firing rate is responsive to derivative D information. Mean spike rate averaged across D-sensitive neurons is shown by the bold line with the shaded region equal to ± 1 standard error. Sensitivity is determined by Kruskal-Wallis test with $\alpha<0.001$. Each colored line is a separate neural unit. (B) From the D-sensitive units shown in A, $n = 18$ units encode D over the entire range of velocities tested (linear regression *t*-test for slope, $\alpha<0.001$). Mean spike rate averaged across D-encoding neurons is shown by the bold line with the shaded region equal to ± 1 standard error. Colors for each unit match those shown in (A).

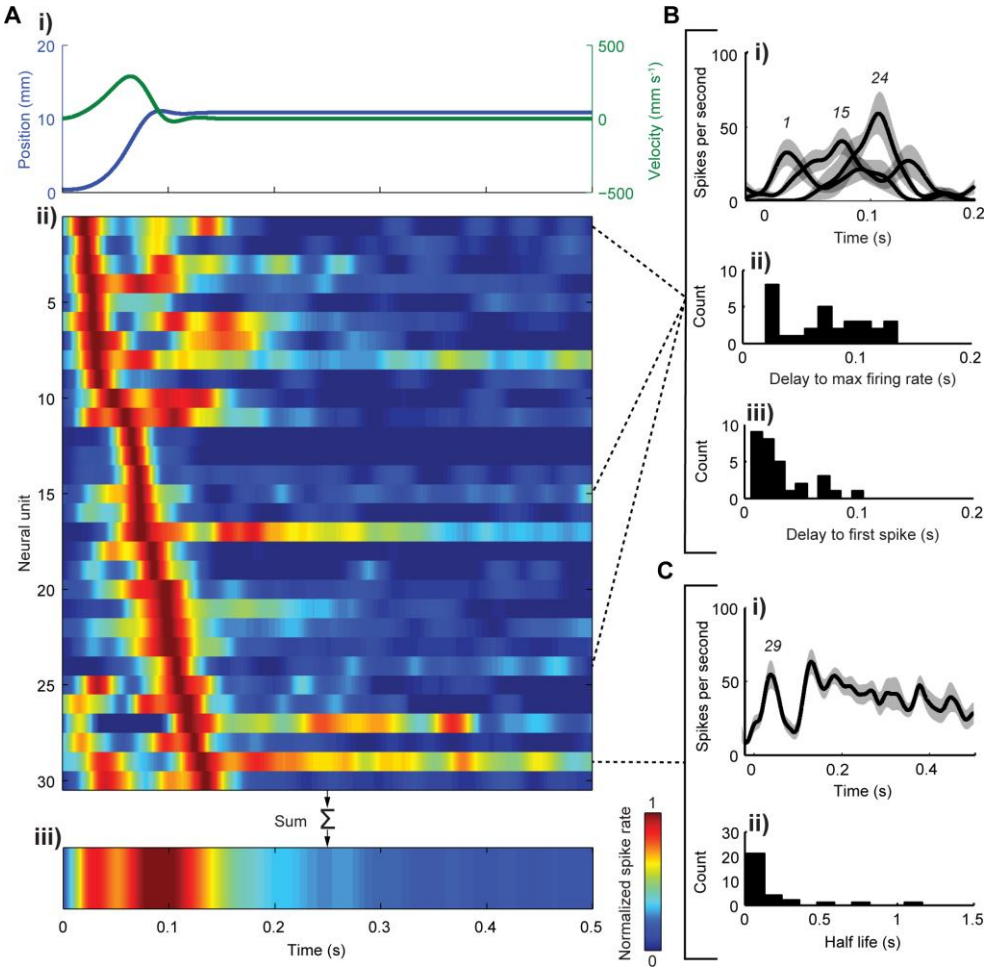

Figure 3. Neural unit temporal processing and summation. (A) (i) Wall position and velocity for fastest-moving wall stimulus (mean velocity = 110 mm s^{-1}; wall moving towards cockroach). (ii) Mean neural Gaussian-convolved firing rates for *n* = 30 D-sensitive neurons from N = 13 individuals (19 recordings total). Unit spike rates are normalized according to their respective maximum spike rate. From top to bottom, neurons are sorted according to their delay to maximum firing rate. (iii) Summation of individual spike rates. (B) (i) Three units (1, 15, 24) are plotted to demonstrate the variation in delay to maximum firing rate (from 10 trials). Histograms show the distribution of delays to maximum firing rate (ii) and first spike (iii) for all D-sensitive neurons. Envelopes are ± 1 standard error around mean firing rates. (C) (i) One unit (29) is plotted to demonstrate slow decay rates (from 10 trials). Envelopes are ± 1 standard error around mean firing rates. (ii) The histogram shows the distribution of half-lives for all D-sensitive neurons.

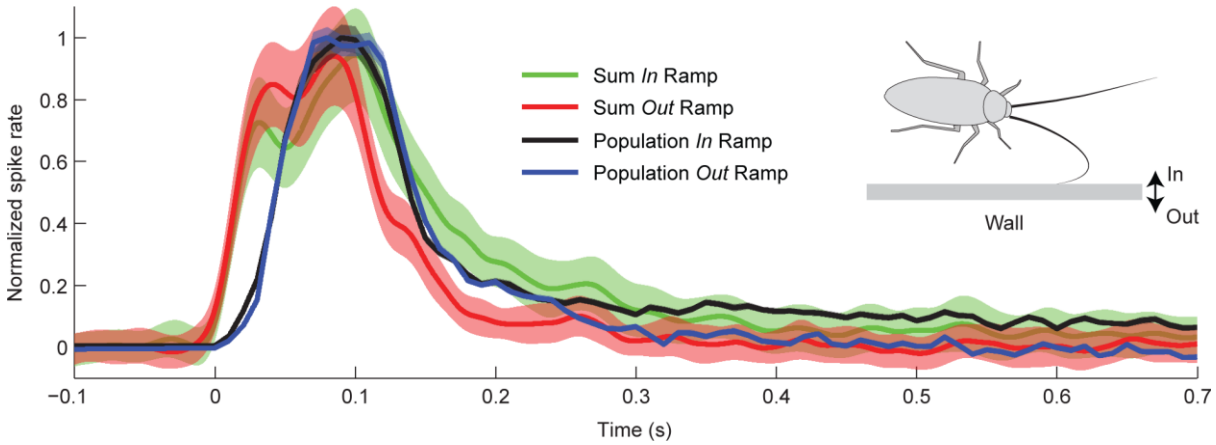

Figure 4. Summation of Gaussian-convolved spike rates for variable-velocity neurons shown in Fig. 3Aii as a function of time for wall moving towards (green) and away (red) from animals (mean velocity = 110 mm s^{-1}). Envelopes are ± 1 standard error. The average root-mean square power of the whole-nerve (population) reported in Lee et al. (2008) is shown for comparison (black: toward animal; blue: away from animal; velocity = 193 mm s^{-1}).

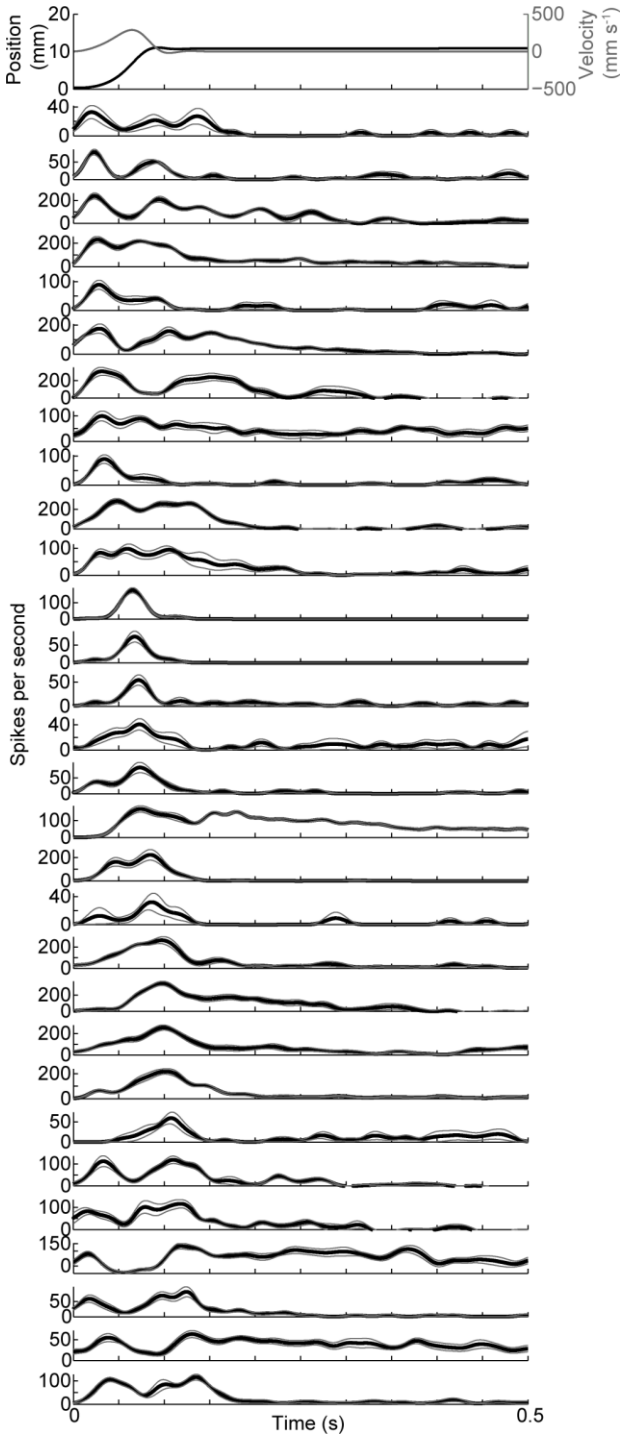

Figure 5. D-sensitive neural units with phasic and phasic-tonic responses. The wall onset is at $t = 0$. Black line are averages and gray lines are ± 1 standard error. From top to bottom, neurons are sorted in increasing order according to their delay to maximum firing rate (same order as Fig. 3Aii).

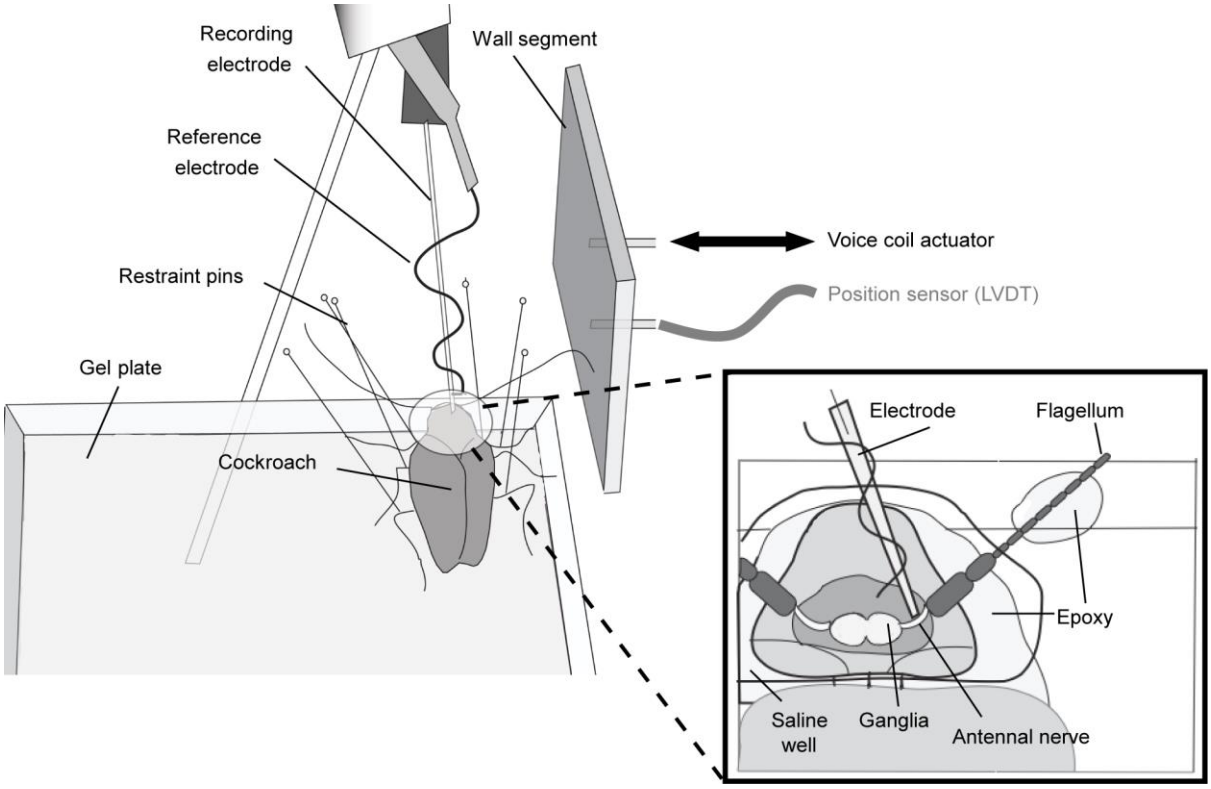

Figure 6. Extracellular recording apparatus. We performed en passant extracellular recordings from the antennal nerve while simultaneously bending the antenna flagellum at prescribed position and velocities with a voice coil actuator to simulate the animal encountering wall projections. A Linear Variable Differential Transformer (LVDT) sensor, mounted in parallel with the actuator, measured the actual position of the wall. We fixed the legs and body of the animal to a platform with insect pins. The head, scape and pedicel segments of the antenna were fixed with glue. The inset shows the recording site at the base of the antenna, relative to anatomical landmarks of the cockroach.

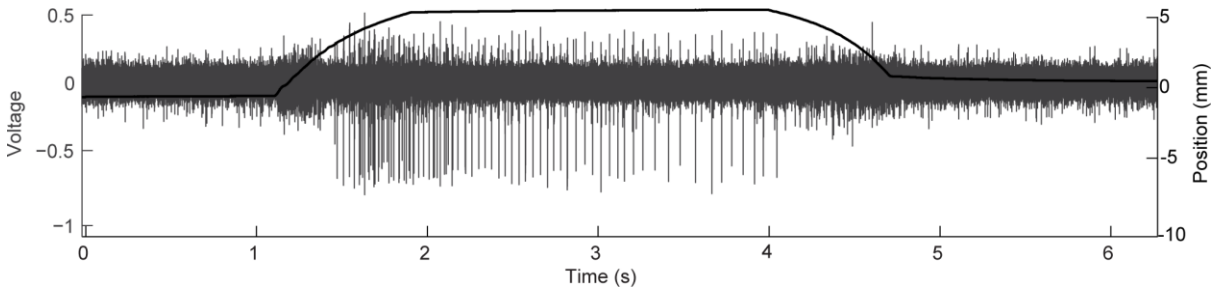

Figure 7. Example of multi-unit extracellular recording (gray) during a ramp-and-hold wall stimulus (black) as a function of time. The neuron with largest amplitude activity shows a characteristic phasic-tonic response.

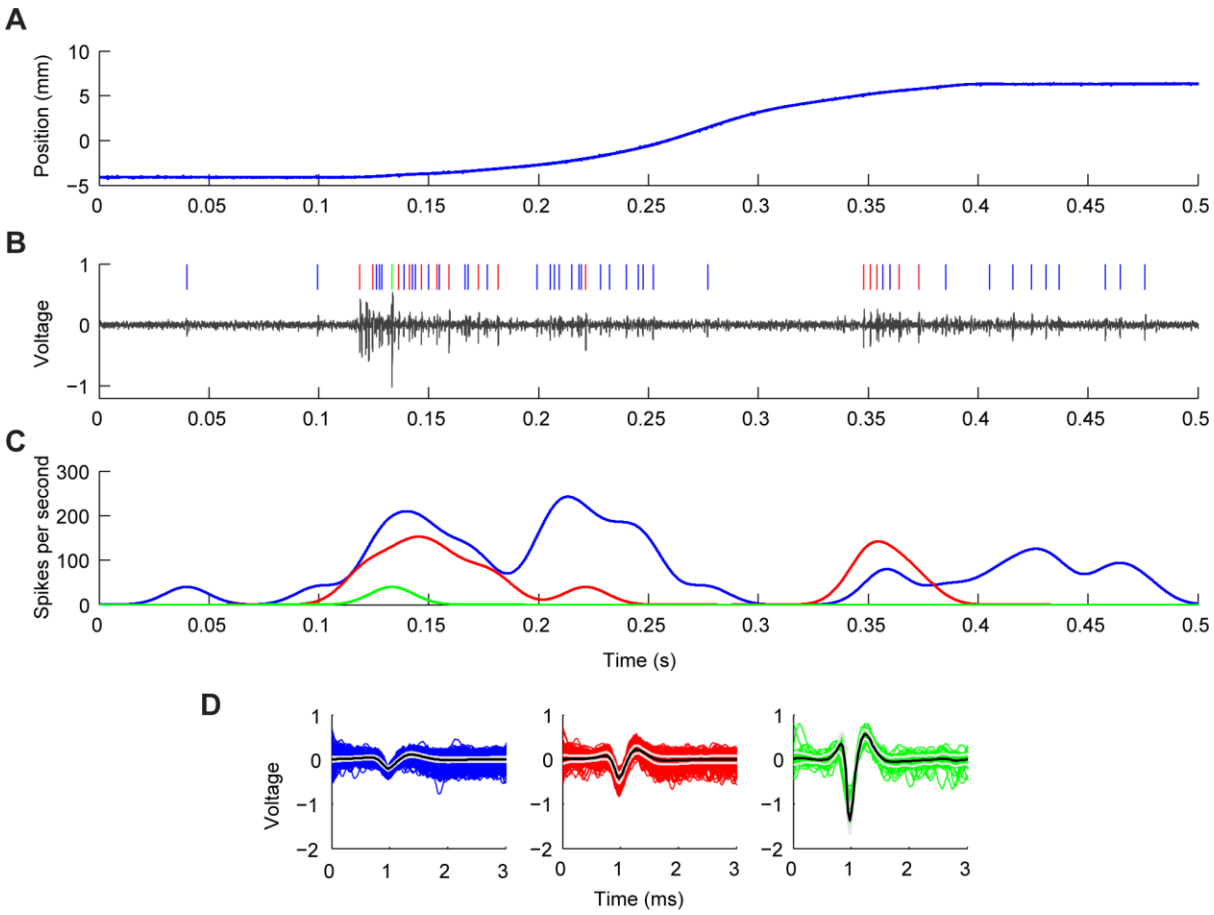

Figure 8. Example of spike clustering for a single wall stimulus presentation. (A) Wall position. (B) Corresponding neural response. We detected individual spikes (vertical line) from the raw neural data (gray). (C) Gaussian-convolved spike rates shown in from individual spikes in (B) Spike rates for three units (blue, red and green) are shown. (D) Spike data from identified clusters from 10 trials from same individual using supervised superparamagnetic spike clustering. The cluster colors represent the three different units identified in (B).